

# Measurement of Nanoparticles True Volume and Density in the Aerosol Phase

C. Jourdain<sup>1</sup>, J. Pongetti<sup>2</sup>, J.P. Symonds<sup>2</sup>, A.M. Boies<sup>1</sup>

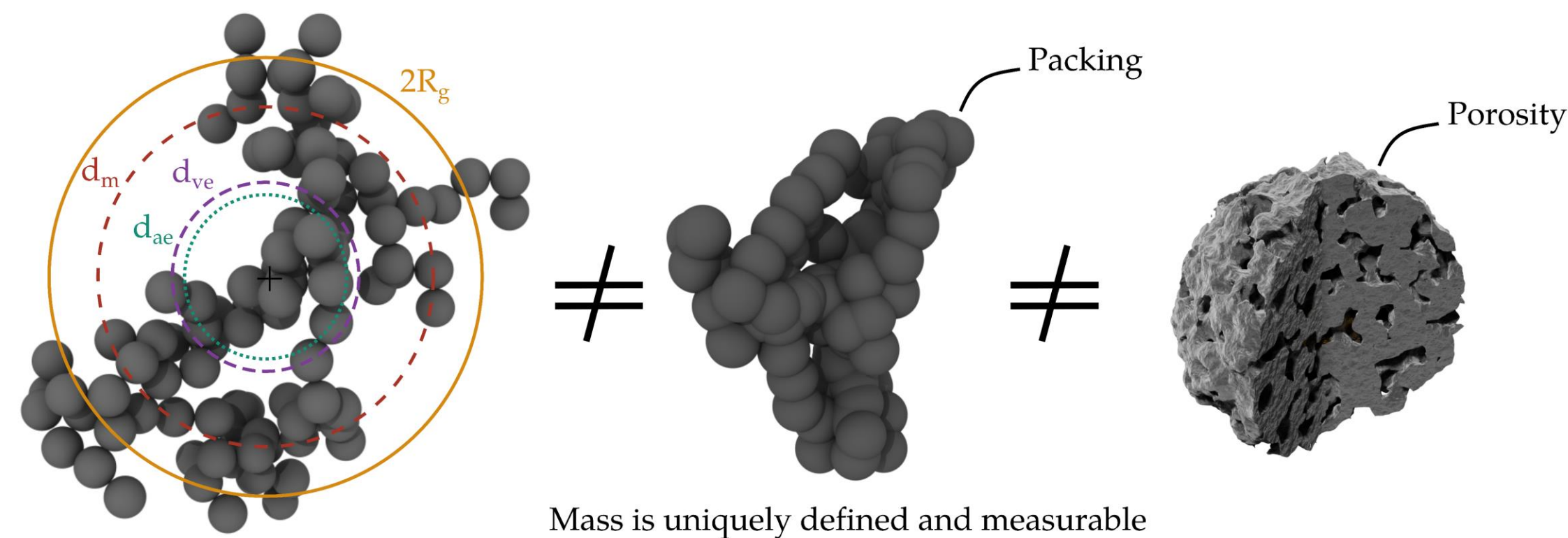


ETH Nanoparticles Conference, June 10-14, 2024



## Background and Motivation

- Fundamental aerosol properties such as volume and density are not known<sup>1</sup>
- True volume is crucial to determining density and derived properties, e.g., porosity<sup>2</sup>, packing factor<sup>3</sup>



- Material density is usually assumed as a constant value from bulk measurements: **What about coated, oxidized, or multicomponent (e.g., bimetallic) nanoparticles?**
- Precise volume and density are required in numerous applications, such as:
  - Nanotechnology and energy (sensors, plasmonics, catalysis, batteries)
  - Aerosol metrology (realistic metrics, standards, calibration)
  - Environment (black and brown carbon, nanoplastics)
  - Health science (cancer treatment, drug delivery)
  - Industry (powders, coatings)
- Current gap:** no technique exists for the direct online measurements of volume and density of nanoparticles

**Objective:** there is an urgent need for developing instruments and techniques that can measure the true properties of nanoparticles as a solid base to further derive secondary properties. This is achieved here by accounting for change in nanoparticles geometry.

**Proposition:** most nanoparticles can be processed at moderately-high temperatures (**condensation technique**), whereas a minority are temperature sensitive, e.g., plastics (**coagulation technique**)<sup>4</sup>

## Condensation Technique



Figure 1: Temperature field (infrared) during warmup.

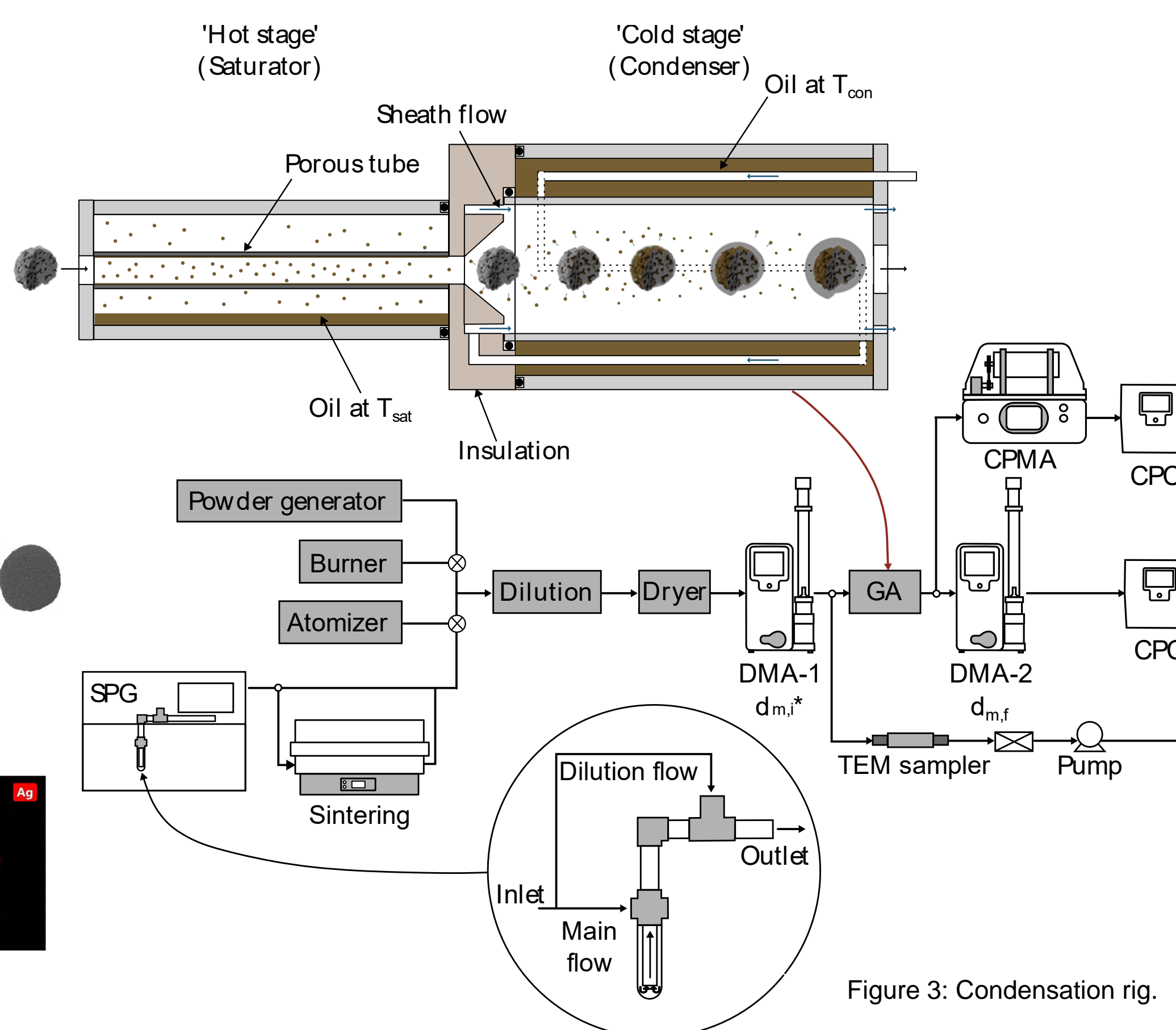


Figure 3: Condensation rig.

- Laminar-flow convective cooling growth apparatus (GA) ( $Le > 1$ )
- Wetted porous tube for maximum inlet saturation uniformity
- Temperature-controlled sheath flow to constrain saturation (and particles) along the axis of the condenser
- High temperature saturator and moderately-high temperature condenser
- Working fluids: heavy oils with low vapour pressure

## Growth Apparatus Simulation

### Incompressible Navier-Stokes

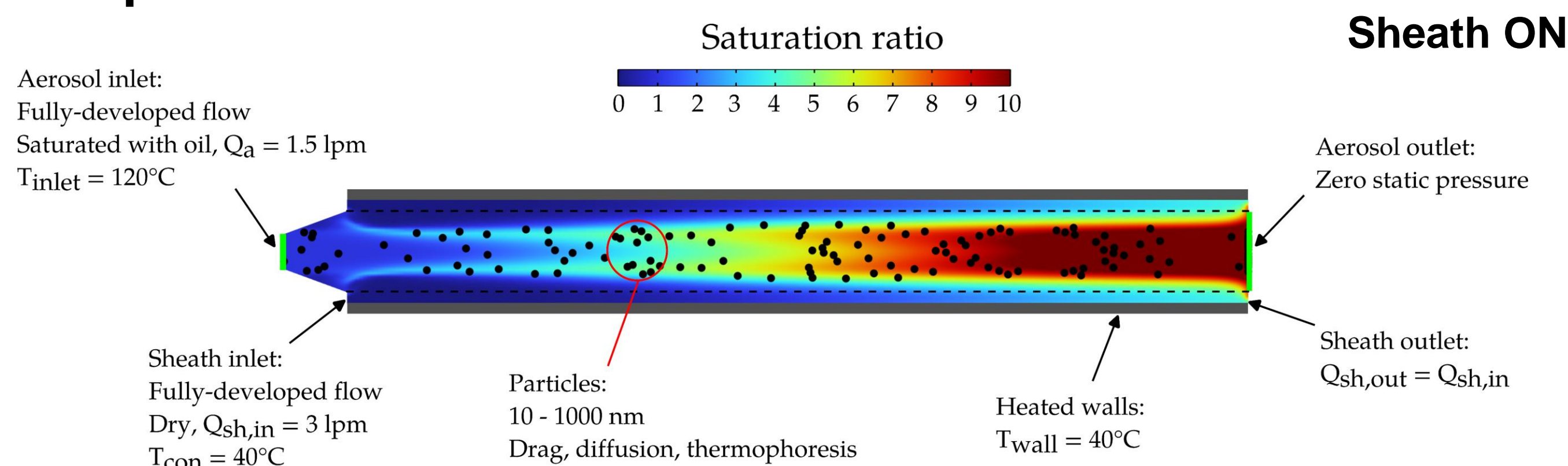


Figure 4: Saturation fields with/without sheath flow (top/bottom)

- Vapour and particles transport in the condenser: solutions for heat and mass transfer coupled with Lagrangian particle tracking
- Supersaturation region along the axis with  $S > 10$
- Diverging section to facilitate activation (pressure gradient)
- Residence time for particles  $\sim 5$  s in condenser
- Assuming that all the vapour condenses on the surface of the particles, the final particle size can be estimated, e.g., 50 nm Ag spheres grow up to 300 nm with  $N = 5.5 \cdot 10^5$  part/cm<sup>3</sup> and  $T_{sat} = 120$  °C



- Vapour diffuses to the walls while smaller particles are lost
- Poorly-controlled growth (due to large variations in residence time) resulting in broader size distributions

## Validation of the Condensation Technique

- Technique was validated using polystyrene nanospheres (PSL) at 220 nm
- Particle growth (mass and mobility diameter) increases monotonically with saturator temperature

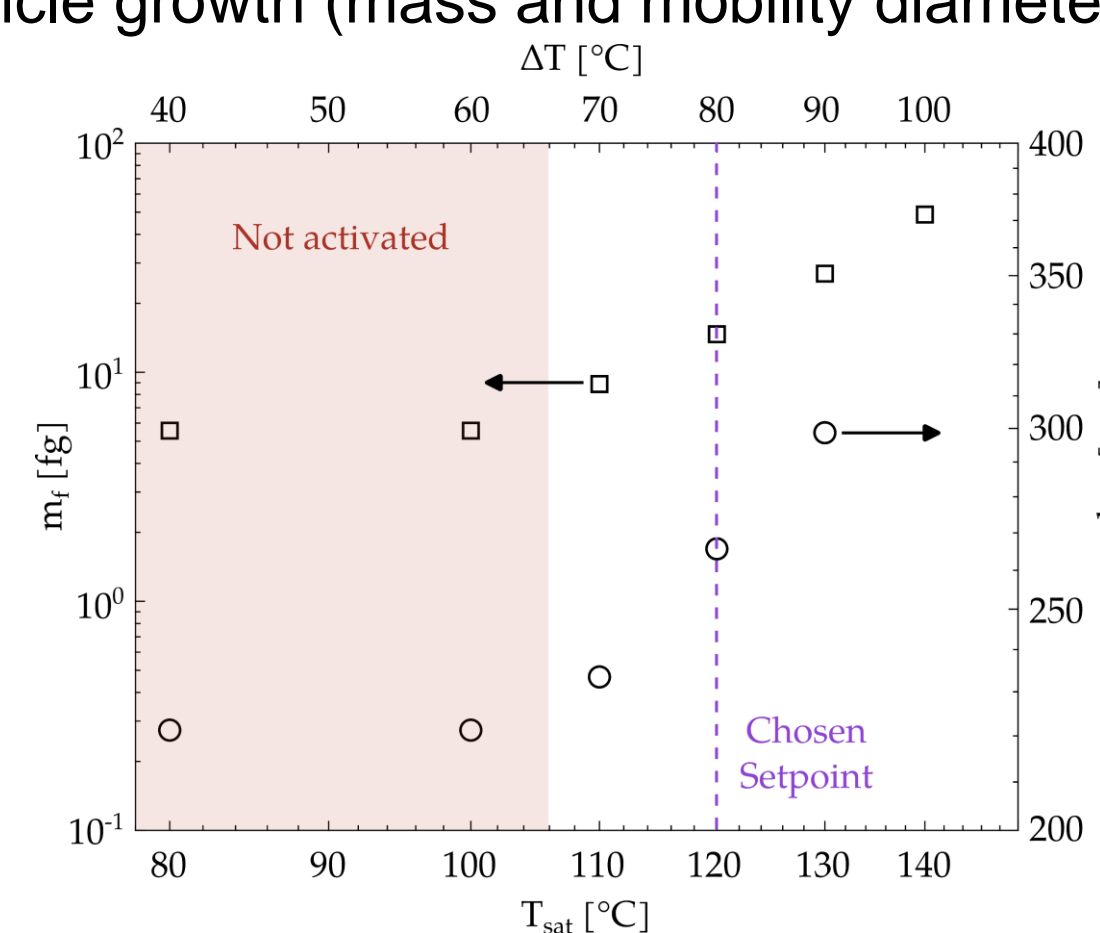


Figure 5: Coated PSL mass (left) and mobility (right) v. saturator temperature.

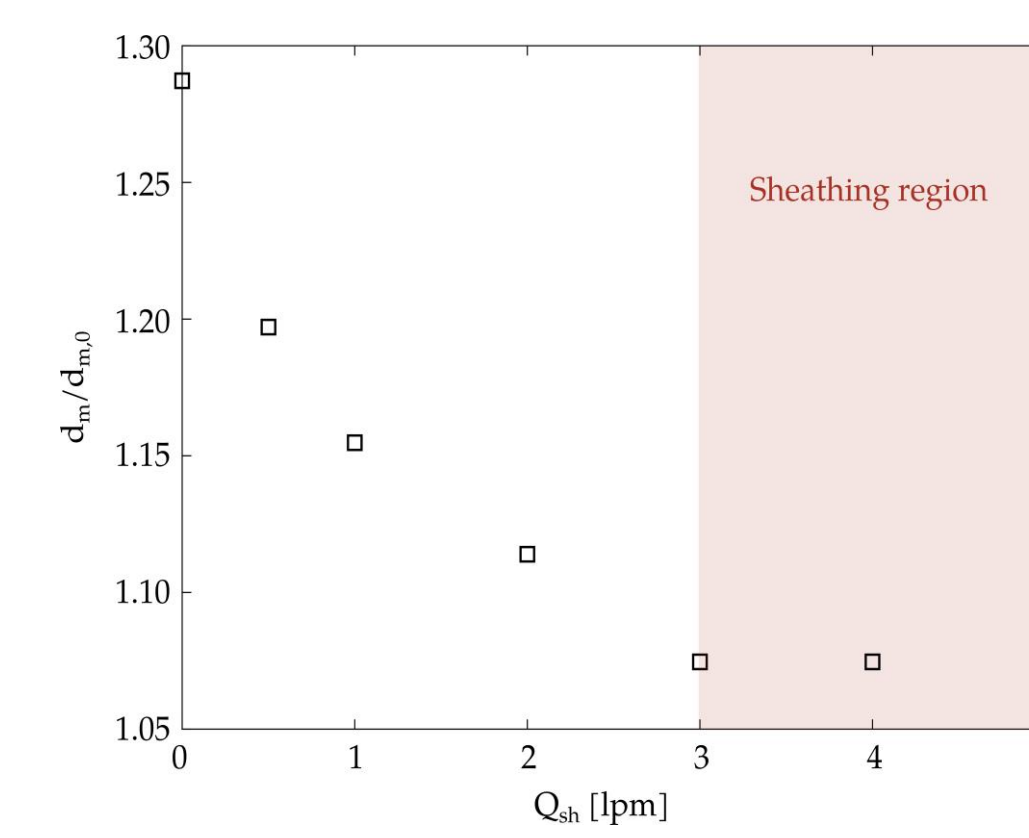


Figure 6: Growth factor v. condenser sheath flow rate.

- Additional sheath flow affects the growth and is crucial for stability: Smaller growth, number concentration, and distribution width due to shorter residence time
- This demonstrates the ability of the instrument to cause condensation on hydrophobic polymer surfaces
- Retrieved values for the volume and density differ by 10.9% and 5.2%, respectively, with the PSL manufacturer-derived values

## Volume and Density Measurement

### Theory and Principles

- (i) Using a very low vapour pressure oil, the coating mass must be conserved
- (ii) A region exists where the particles grow radially, i.e., as spherical droplets

$$(m_f - m_i) = \left( \frac{\pi}{6} d_{m,f}^3 - V_s \right) \rho_c \quad \text{and} \quad \chi_f = \frac{d_m C_{ve}}{d_{ve} C_m} = 1$$

change in mass = mass of coating

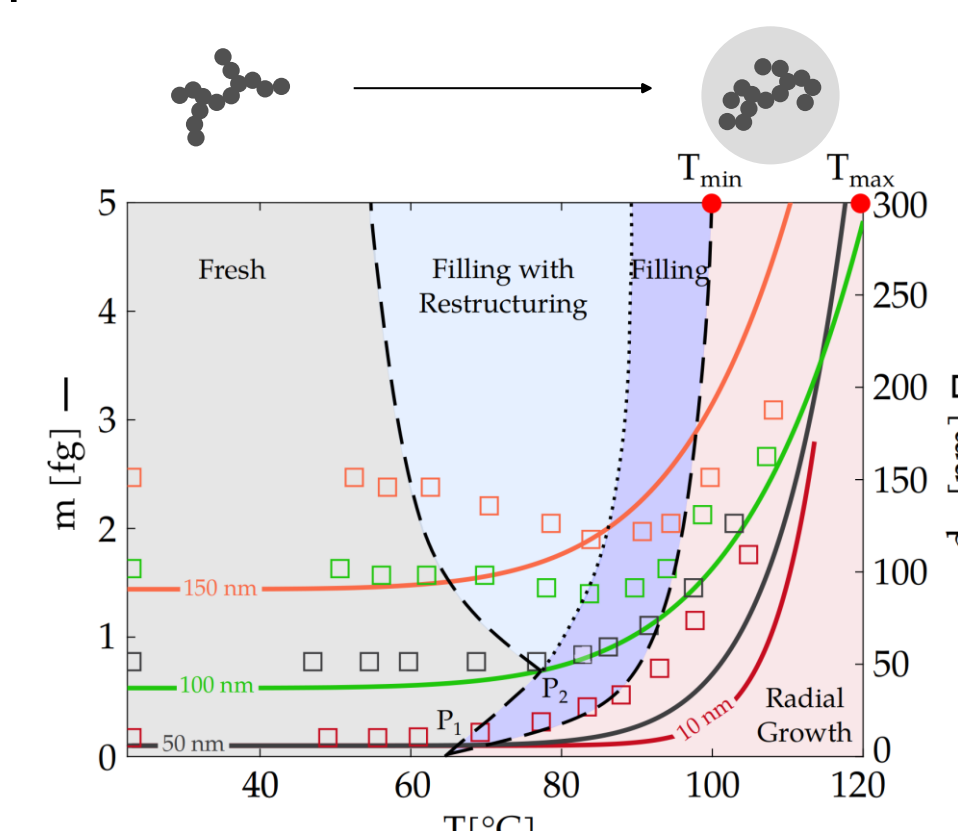


Figure 7: Growth of silver aggregates in mass and mobility with saturator temperature.

### Processing of Ag Aggregates

- Triple point (P2) separates the multi-stage condensation
- $T_{sat}$  is set in the region  $[T_{min}, T_{max}]$
- Filling mechanisms include *Ab initio* cluster and islands formation (pore adsorption, pendar rings) Surface diffusion and film formation v. droplet growth (hydrophobic)

### Volume/Density of Ag Nanoparticles

- Relationship between  $V_s$  and  $d_{m,i}$  for Ag aggregates is  $V_s = 3.75 d_{m,i}^{2.48}$
- Average true density of Ag aggregates is obtained from the slope of the  $(m_i, V_s)$  curve and can reach down to  $\sim 2,000$  kg/m<sup>3</sup>, which agrees with the density found for Ag primary particles<sup>5</sup>
- Large overestimation of volume using spherical approximation
- Surface area is derived using the true volume according to semi-empirical relations<sup>6</sup>
- Size-dependent packing factor: 0.47 (135 nm) to 0.89 (57 nm)
- Size-dependent porosity is estimated using the effective density (from mass-mobility): 54% (135 nm) to 11% (57 nm)
- Small sintered Ag aggregates have also been measured:  $V_s = 1.4 \cdot 10^3$  nm<sup>3</sup> (20 nm),  $6.2 \cdot 10^3$  nm<sup>3</sup> (30 nm),  $7.9 \cdot 10^3$  nm<sup>3</sup> (40 nm). The retrieved density ( $\sim 11,000$  kg/m<sup>3</sup>) is higher than both the oxidized and pure states of silver possibly due to changes in lattice parameter during sintering

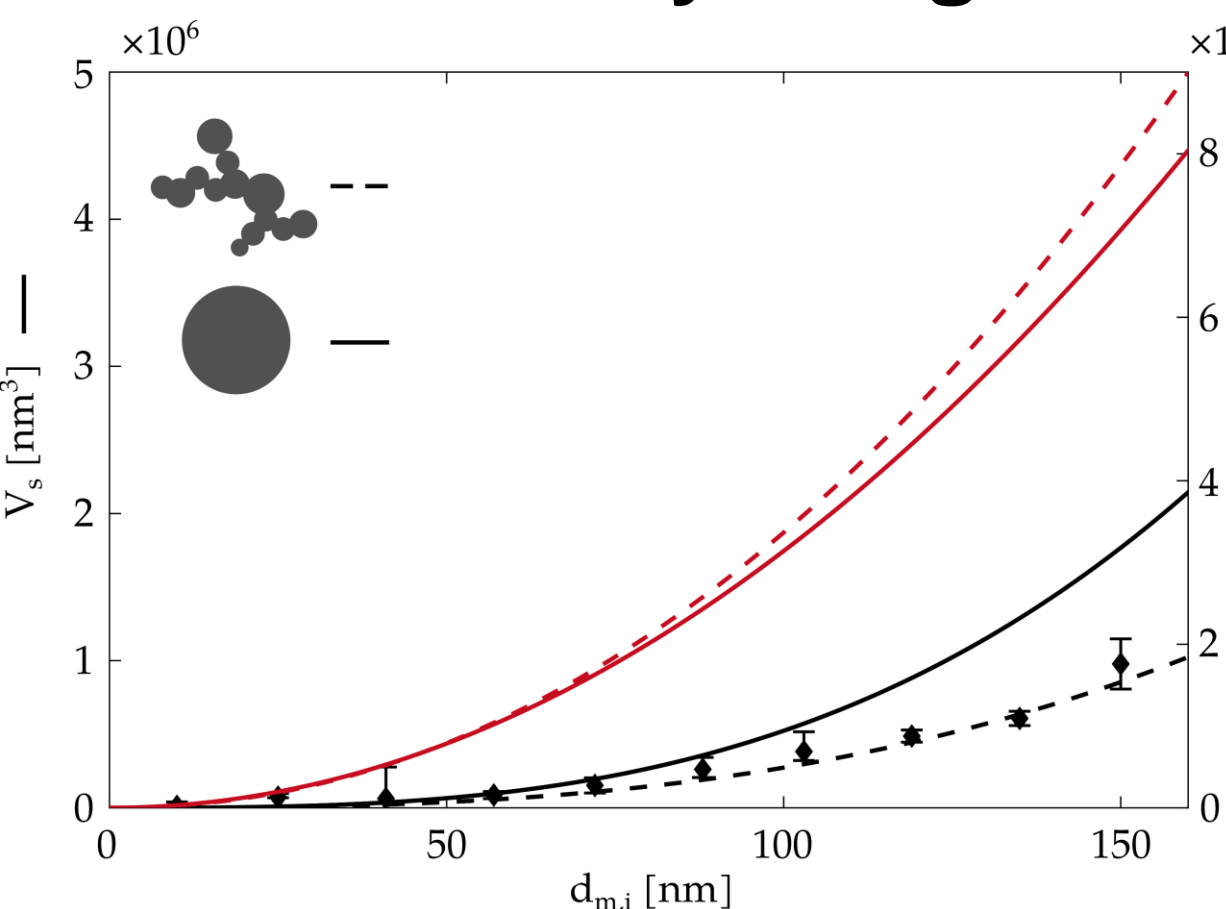


Figure 8: True volume ( $V_s$ ) and surface area (SA) of Ag aggregates and spheres v. initial mobility diameter ( $d_{m,i}$ ).

## Feasibility of a Coagulation Technique

### Principles and Setup

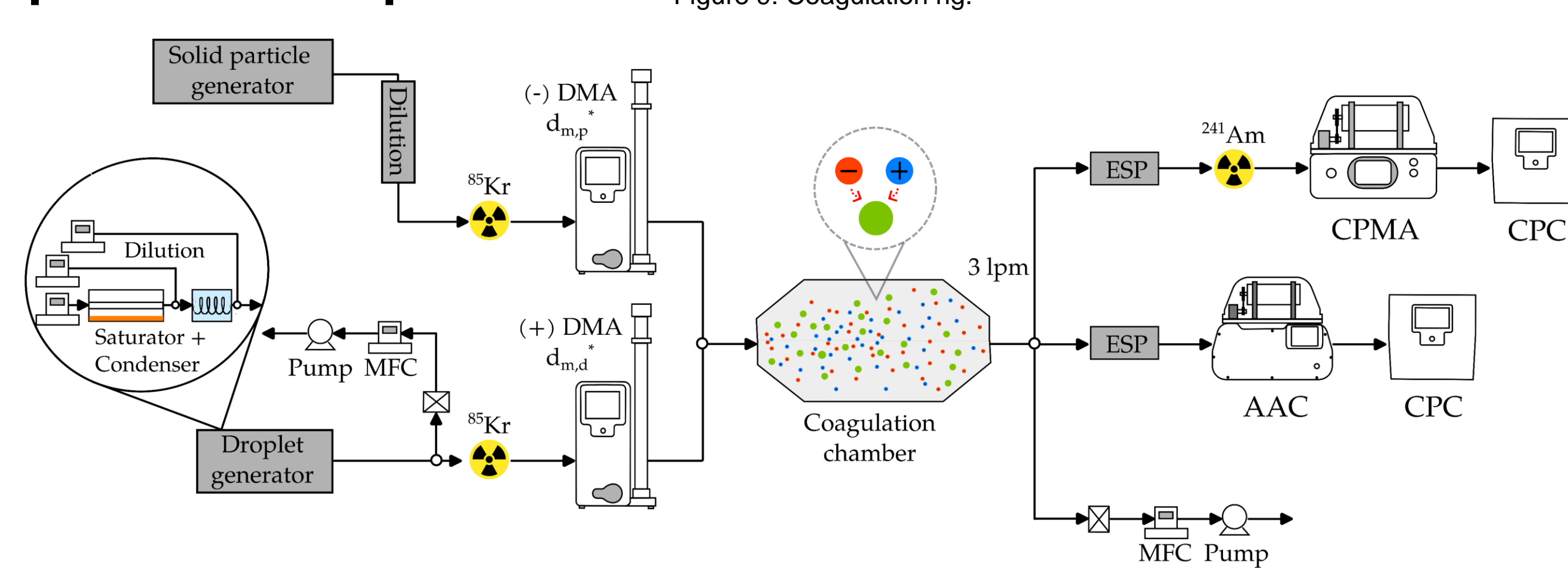


Figure 9: Coagulation rig.

### Particle-Droplet Collision

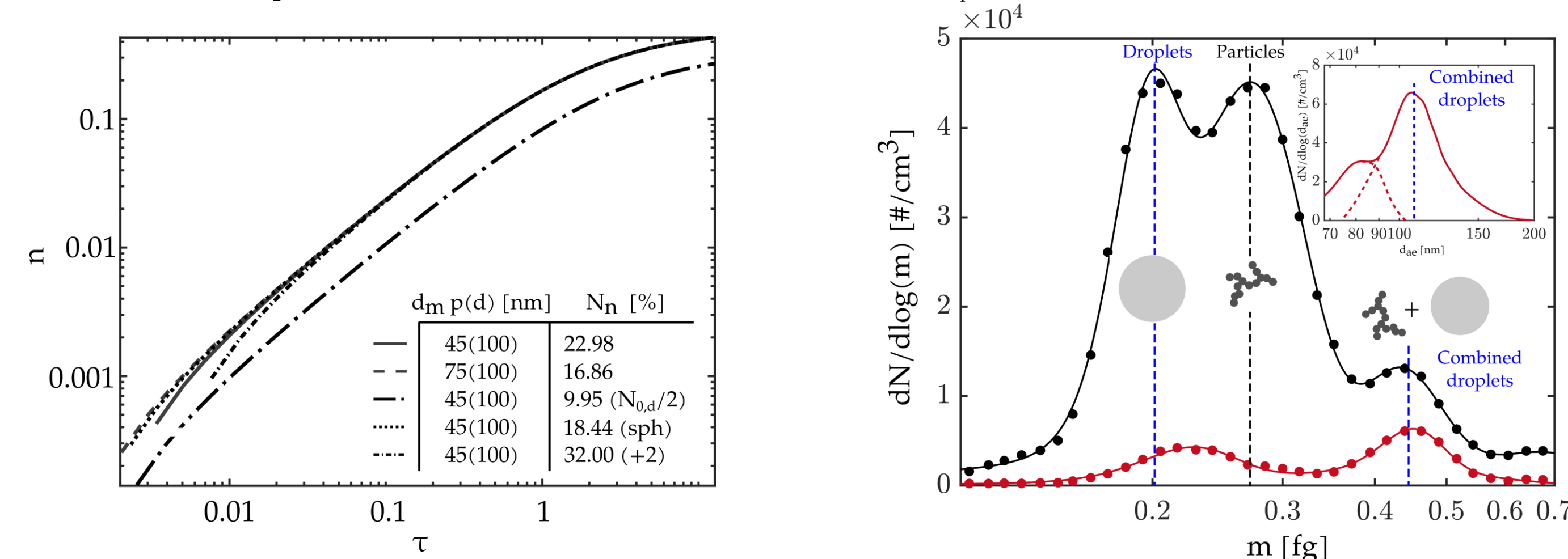


Figure 10: Modeled non-dimensional collision kernel components.

Figure 11: Mass and aerodynamic spectra of attached particles-droplets.

- 0-D collision model used to design the coagulation chamber and choose the experimental setpoints
- Mono-mobile droplets and particles shown to 'attach' via joint electrostatic and Brownian interactions
- Sticking coefficient assumed unity, however the collision v. coagulation kinetics need further investigation

## References

- Sipkens T. *et al.*, *J. Aerosol Sci.*, **173** (2023)
- Zangmeister C. D. *et al.*, *PNAS*, **111**, 25 9037-9041 (2014)
- Lee S.Y. *et al.*, *Carbon*, **49**, 7, 2163-2172 (2011)
- Jourdain C. *et al.*, *in preparation* (2024)
- Schleicher B. *et al.*, *J. Appl. Phys.*, **78**, 4416-4422 (1995)
- Eggersdorfer M. L. *et al.*, *J. Aerosol Sci.*, **46**, 7-19 (2012)

## Funding and Contact

C.J. is supported during his PhD by Cambustion Ltd and EPSRC grant 2434524. C.J. acknowledges the financial contribution of the Cambridge University Department of Engineering. C.J. thanks Zoran Hadzjivanov (Cambustion) for generating the powder images using Blender.

Contact: [cj443@cam.ac.uk](mailto:cj443@cam.ac.uk)